This article has been accepted for publication in IEEE Open Journal of the Industrial Electronics Society. This is the author's version which has not been fully edited and content may change prior to final publication. Citation information: DOI 10.1109/OJIES.2023.3290169

Digital Twin-Based Diagnosis and Tolerant Control of T-type Three-level Rectifiers

Ali Sharida[1,2], Student Member, IEEE, Naheel Kamal[1,2], Student Member, IEEE, Hussein Alnuweiri[2], Senior Member, IEEE, Sertac Bayhan[3,4], Senior Member, IEEE, and Haitham Abu-Rub, Fellow[2], IEEE

[1]Texas A&M University, College Station, USA
[2]Texas A&M University at Qatar, Doha, Qatar
[3] Qatar Environment and Energy Research Institute, Hamad Bin Khalifa University, Qatar
[4] Gazi University, Ankara, Turkey
Corresponding author: Ali Sharida (e-mail: ali.sharida@ qatar.tamu.edu).

ABSTRACT This paper proposes a digital twin-based diagnosis and fault tolerant control for T-type three-level rectifiers. To develop the digital twin (DT), a dense deep neural network (DNN) machine learning approach is used. The digital twin is trained offline using a set of experimental data and updated online to get the maximum possible accuracy. Then, the DT is used for the diagnosis and tolerance of open-switch faults (OSFs) and faults related to voltage and current sensors (VACSF) or for sensorless control. The open-switch fault detection and localization algorithm is implemented based on the dynamic response difference between the physical system and its digital twin. First, the open-switch fault is detected and localized based on the grid current dynamics, where each switch fault generates a specific pattern in the current dynamics. Open-switch fault is tolerated by changing the switching function based on the location of the fault. Second, the voltage and current sensors fault is detected when the digital twin provides a specific amplitude of currents while the physical sensors do not provide a correct measurement. This case is tolerated by feeding back the grid currents or voltages from the digital twin as an alternative to the physical sensors. The proposed technique has low overhead, enhances the reliability of the power converter, and is applicable for sensorless mode of control. Experimental investigations are conducted to validate the proposed concept.

INDEX TERMS Digital twin, open-switch fault detection, sensors fault detection, fault-tolerant control, sensorless control.

I. INTRODUCTION

A Digital Twin (DT) refers to a computer-generated copy of a tangible entity, such as a machine or a power converter. The key benefit of a DT lies in its ability to simulate and evaluate the functionality and actions of the actual asset in a digital realm. This can provide several benefits, including (i) predictive maintenance: by simulating the asset's performance in a virtual environment, which makes it possible to predict when maintenance or repairs are needed, allowing for proactive maintenance, and reducing downtime; (ii) improved design: a DT can be used to test and optimize the design of the asset before it is built, allowing for improvements in performance and efficiency; (iii) increased understanding: DTs can provide a detailed understanding of how asset functions, which can be used to identify potential problems and improve the performance; (iv) remote monitoring and cyber-physical security: DT can be connected to the real-world asset, allowing for remote monitoring, cyber-physical security, and control of the asset; (v) cost savings: by using a DT to co-simulate and analyze the performance of an asset, it is then possible to reduce the costs associated with testing, maintenance, and repairs.

DT is an emerging technology that is being increasingly used in many fields such as monitoring systems, 3D models, Internet of Things (IoT), Transfer Learning (TL), Artificial Intelligence (AI), distributed computing, mobile communications, Augmented Reality (AR), Virtual Reality (VR), and electronic sensors [1]. Recently, DT has become widely spread in smart grid applications in general and for power electronics converters in particular [2-5]. DT has been used as a replica of a modular multi-level converter in [2], where the DT was implemented on a real-time controller and served as hardware in the loop simulator. In [3], the DT was employed for fault diagnosis approach for distributed photovoltaic system connected to a DC-DC power converter. The difference between the DT outputs and physical measurements is analyzed to generate an error residual signal that can be used to judge the state of operation of the system. DT was also used for online diagnostics of power converters [4], where the behavior of the physical converter is continuously compared with the behavior of the DT to make sure that the physical converter is working well. However, this method indicates only if the converter is working well or not and does not provide any details about the type or the location of the fault. In [5], the DT was designed using particle swarm optimization algorithm, and was used as a replica of a buck DC-DC converter for observing the degradation trends of the physical components such as capacitors and power switches. To sum up, DT is used in power converters as hardware in the loop simulator, system monitoring, passive components trend degradation, and as an indicator for power converter's state of operation. However, DT has not been utilized yet as a fault detection, fault localization, and fault tolerant control technique.

Fault detection and tolerant control become a requirement in the industrial power converter applications where the reliability is crucial. In general, power converters are exposed to multiple possible faults that threat the operating system's reliability. Most of these faults occur due to the power switches as they are fragile components and may fail due to the transient currents or voltages. The failure of a power switch causes higher currents to flow through the circuit and through the other switches, which may cause a fatigue failure in the entire system. Sensor faults are also common in power converters which occur usually due to the harsh environment (high temperature and humidity), surrounding electromagnetic fields, and possible attacks [6]. Sensors faults deteriorate the response of the control process leading to multiple severe problems such as high steady state error, decreased power factor, and deteriorating power quality.

This work is licensed under a Creative Commons Attribution 4.0 License. For more information, see https://creativecommons.org/licenses/by/4.0/

This article has been accepted for publication in IEEE Open Journal of the Industrial Electronics Society. This is the author's version which has not been fully edited and content may change prior to final publication. Citation information: DOI 10.1109/OJIES.2023.3290169

Therefore, the availability of the system and the control algorithm to operate in case of switches and sensors is essential from the reliability point of view. Therefore, faults detection and tolerant control become essential requirements for reliability enhancement.

In literature, different methods were proposed to detect and localize such faults. For example, open-switch fault was detected and localized using online machine learning algorithm (OMLA) [7]. However, OMLA is difficult to implement on an embedded system or a low-cost microcontroller. Total harmonic distortion (THD) [8] and current distortion [9] are among the most widely used methods to detect and localize the OSF. In fact, the computation of the distortion or the THD of three-phase currents is time consuming and requires high-speed and high-accuracy data acquisition. This increases the complexity and the cost of the fault detection system. In [10], the fault-assumed strategy was used for OSF detection, where the computed voltage based on the switching states and the fault-assumed-based voltage are compared and analyzed to detect the OSF. However, the measurement or the estimation of the poles' voltages are required for this method. Therefore, either extra three-sensors are required, or the complexity and computational load will be increased due to the complexity of the pole's voltage estimation. In [11], the phase angle value was combined with the instant when the grid current is zero to pinpoint the fault. This method requires fast and real-time current measurements to detect the correct instant when the grid current is zero. Missing the zero-current instant will cause the fault detection to be delayed until the next cycle or the results of the detection will be incorrect since distinct switch faults have slight phase angle variations.

For sensor faults problems, multiple sensorless control and states estimation methods have been investigated for grid voltages and currents [12], [13]. One of the most popular methods for grid voltage estimation is virtual flux (VF) [14], where the VF vector is constructed using an ideal integrator. However, in practical application, the dc drift and the initial bias are the main limitations of a pure integrator. These problems are usually addressed by using a low-pass filters or a second-order generalized integrators. However, a long delay may occur during transient process (like startup or sudden voltage change) if these filters were employed in an open-loop estimator. State feedback observers (SFO) [15] and Luenberger observer [16] can also be used for grid voltage estimation which have closed-loop estimator, unlike VF. However, SFO completely depends on the mathematical model (State space) of the system, any uncertainty in model's parameter will deteriorate the accuracy of the observer. Moreover, sensors faults tolerant method is proposed in [6] for both current and voltage sensors based on Kalman filter algorithm (KFA). KFA was employed to estimate grid voltages based on the available current measurements and vice-versa. However, KFA suffers from parameter initialization, high starting overshoot, and error variance and covariance matrices selection. Sliding-mode observers are rarely used for grid voltage estimation [17] as they are exposed to high-frequency chattering especially under abnormal conditions such as unbalanced and distorted grid voltages. On the other hand, a load currents estimator is proposed in [13] based on rectifier's mathematical model. However, this method requires the measurements of both grid voltages and current to estimate the load current at the DC side. A look-up table was employed in [18] to perform current sensorless control. Despite that the look-up table has a simple structure and is compatible with low-cost microcontrollers, it is not suitable for fast-dynamics applications that are exposed to noises and disturbances. Current reconstruction and mathematical model-based compensations methods are widely spread for current sensorless control [19]. However, these methods depend on determining the exact mathematical model which is difficult to be obtained in a practical application. Therefore, the estimation error is the main limitation for such methods especially under the existing of noises and uncertainties. All of the mentioned problems can be overcome by using DT-based fault detection and fault tolerant techniques.

Machine learning (ML) and deep neural networks (DNN) have been used in many fault detection and system modeling applications [20]. Recurrent Neural Networks (RNN) is one of the most common ML methods that offer internal memory in their neurons. This is helpful when the application considers past events in the prediction like in timeseries problems [21]. Convolutional Neural Networks (CNNs), on the other hand, are often used for two-dimensional inputs like images, but also with a single-dimensional variant [22]. However, CNN has no memory of past events. Temporal Convolutional Networks (TCNs) combine the ideas of RNNs with a single-dimensional CNN offering even higher performance [23]. One major issue with all the aforementioned methods is the high computational complexity. For the model to be applicable in the proposed application, it needs to be deployed on a low-cost microcontroller and to function with minimal time overhead. Unlike the previously mentioned DNNs, basic dense, fully connected, DNNs can be built to fit in a computationally limited device while offering relatively accurate predictions, which are used in this work.

Existing fault tolerant control techniques in literature have major limitations in the realm of open-switch faults and measurement sensors faults. These limitations include high computational power, complex designs, reliance on costly redundant components, compatibility with only specific types of faults, the need for additional sensors, high-cost measurement acquisition systems, and dependence on precise time measurements during zero-current instances. Consequently, these limitations restrict the applicability of such methods in industrial applications where low-cost microcontrollers are typically employed.

Hence, it becomes imperative to develop a unified algorithm that enables systems to detect and tolerate open-switch faults, voltage sensor faults, current sensor faults, and facilitates sensorless control of voltage and current. Furthermore, there are other important objectives to be achieved, including grid current regulation, DC link voltage control, balancing of DC side capacitors, enhanced power quality, minimized tracking error and overshot, increased robustness against parameters discrepancies, as well as resilience against weak grid conditions and abnormal grid situations. Consequently, the motivation behind this paper lies in introducing a comprehensive solution that addresses all of these challenges collectively. The proposed algorithm relies on the principle of the digital twin (DT), which acts as a replica of the physical system under normal conditions.

This article proposes novel DT-based methods for open-switch faults detection and localization, grid voltage and current sensors fault tolerant control. These methods are applied to a

This work is licensed under a Creative Commons Attribution 4.0 License. For more information, see https://creativecommons.org/licenses/by/4.0/

This article has been accepted for publication in IEEE Open Journal of the Industrial Electronics Society. This is the author's version which has not been fully edited and content may change prior to final publication. Citation information: DOI 10.1109/OJIES.2023.3290169

three-level three-phase T-type rectifier as a case study. The proposed methods have the advantages of simplicity, lower computational burden, applicability for low-cost microcontrollers, comprehensively against all kinds of faults, reliability, and have higher accuracy. Moreover, the proposed sensor faults tolerant algorithm is applicable for both voltage and current sensors faults. The currents generated from the DT are used as alternatives to the current sensors in case of current sensors faults, while the inverse of digital twin is used to estimate grid voltages in case of voltage sensors failure. Finally, the proposed open-switch fault detection algorithm can detect and localize the faults within a short period (10ms). The main contributions of this paper are summarized as follows,

1. Novel design of a DT for three-phase three-level T-type converter: The DT is designed offline to minimize computation time and is further enhanced online to improve the efficiency and reliability of the proposed solution.
2. Novel design of open-switch fault diagnosis and tolerant control: This method provides the advantages of simplicity and eliminates the need for additional components such redundant switches or extra sensors. It exhibits a rapid response, enabling the detection, localization, and tolerance of faults rapidly.
3. Novel design of voltage and current sensors faults diagnosis and tolerant control, including sensorless control: This method significantly enhances the reliability of the entire system when sensor-fault tolerant control is employed, and reduces system's costs when sensorless control is implemented.

II. MODELLING, DIGITAL TWIN DESIGN, AND CONTROL OF T-TYPE RECTIFIER

A. Modeling and digital twin design

The circuit diagram of a T-type rectifier is shown in Fig. 1a. It consists of three-legs connected to the grid through an input filter that has inductance (L_g) and resistance (R_g). The AC side dynamics for this topology is given by,

$$\mathbf{V}_{abc} = L_g \frac{d\mathbf{I}_{abc}}{dt} + R_g \mathbf{I}_{abc} + \mathbf{U}_{abc} \quad (1)$$

where $\mathbf{V}_{abc}$, $\mathbf{I}_{abc}$, and $\mathbf{U}_{abc}$ are the grid voltage, grid currents, and the rectifier's input voltage. SXY represents the gate of each switch, where $X \in [1\ 2\ 3\ 4]$ and $Y \in [A\ B\ C]$.

Eq. (1) is used to provide the initial model of the DT as shown in Fig. 1b. The DT receives the physical measurements of rectifier's inputs, namely grid voltages ($\mathbf{V}_{abc}$) and the control signals ($\mathbf{U}_{abc}$). These measurements are then used to compute rectifier's outputs, namely grid currents ($\mathbf{I}_{abc}$) and the DC link voltage (V_{dc}). Initially, the values of passive parameters are set by default to 1mH, 1mΩ, and 20Ω for the input filter inductance, input filter inductor's resistance, and the load resistance respectively. Then, these parameters are updated using machine learning (ML) techniques. When the ML model is trained, the obtained model is used as a DT for the T-type rectifier.

To train the ML model, data has to be first collected from real hardware measurements. A lab-scale experimental setup was used to collect 81,561 measurements while varying the load and the reference DC Voltage (V_{dc}^*). V_{dc}, $\mathbf{I}_{abc}$, $\mathbf{V}_{abc}$, and $\mathbf{U}_{abc}$ were collected from the controller and used to build the dataset. Collection of the data is performed using the STM Studio software communicating with ST-Link compatible hardware for debugging the code on the microcontroller. Measurements gathered from the sensors are stored on compile-time defined addresses on the microcontroller's memory. These memory locations are accessed at run-time using the STM Studio debugger and are stored as log files. To vary V_{dc}^*, the memory address of V_{dc}^* is set to be writable from the debugger and is changed at different times. To vary the load, a programmable load is used with a wide range of different values. After the data collection step, the log files generated from the STM Studio are parsed and combined to build the dataset.

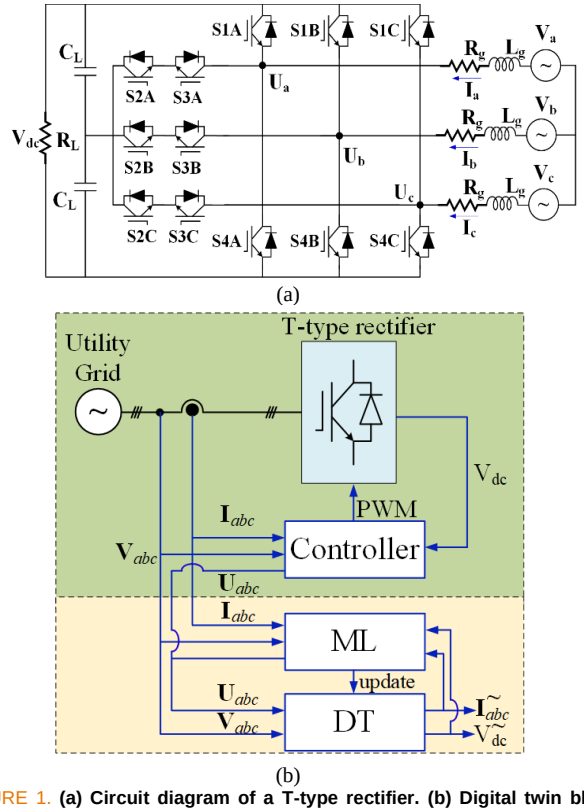


FIGURE 1. **(a) Circuit diagram of a T-type rectifier. (b) Digital twin block diagram.**

The dataset is processed to train a fully connected dense deep neural network model as shown in Fig. 2. The model is composed of three hidden layers, a 6-units input layer, and a 4-units output layer. The number of the units of the input and output layers is chosen to reflect the proposed DT model inputs and outputs. Given the proposed fully connected architecture, the model manages to predict $\mathbf{I}_{abc}$ and V_{dc} accurately with minimal computational time.

The ML model is trained offline and updated online using the TensorFlow (TF) library on a local PC and then deployed on a low-cost microcontroller using TensorFlow Lite Micro (TFLM). Unlike typical DNN-based systems, the trained model is optimized and compiled to low-level machine code with TFLM. The generated model occupies approximately 30KB of the microcontroller's flash memory, and the inference of a single instance takes around 7µs. Furthermore, the measurement acquisition process requires 2-4µs, while the control algorithm itself requires nearly 3µs. These characteristics make the proposed machine learning model highly suitable for integration into the control system, as it does

This work is licensed under a Creative Commons Attribution 4.0 License. For more information, see https://creativecommons.org/licenses/by/4.0/

This article has been accepted for publication in IEEE Open Journal of the Industrial Electronics Society. This is the author's version which has not been fully edited and content may change prior to final publication. Citation information: DOI 10.1109/OJIES.2023.3290169

not excessively consume the limited available hardware resources specified for the system's operation.

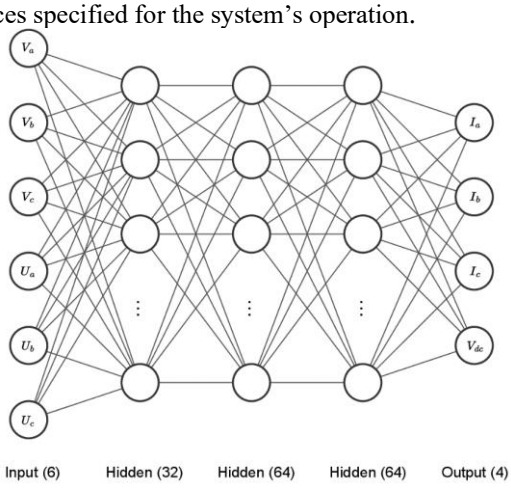


FIGURE 2. **Adopted ML DNN architecture.**

To ensure optimal training of the machine learning (ML) model, the collected dataset is divided into 80% for training purposes and 20% for validation. Following 100 epochs of training, the mean absolute error (MAE) for the validation data reaches 0.7. The validated predicted curves are compared to the corresponding physical values, as depicted in Figures 3a and 3b for the steady state, and Figures 3c and 3d for the transient period.

To evaluate the accuracy of the trained model, the mean square error (MSE) is computed over a single cycle. During the steady state, the training MSE error amounts to approximately 0.09A for the grid currents and 0.93V for the DC link voltage. However, during transient periods, the MSE temporarily increases to 0.23 for the grid currents and 2.75V for the DC link voltage. This increase is attributed to the fact that the DNN model reacts slightly faster to changes compared to the physical system, due to the dense model nature lacking memory of past events.

The training process of the DC link voltage is validated using multiple voltage levels, as demonstrated in Fig. 4. The MSE over the entire period amounts to 0.57V. From a perspective standpoint, the mean absolute percent error remains at 0.85% in the worst-case scenario during the transient period, specifically during the voltage transition from 90V to 100V. This indicates that the proposed ML-based DT model is capable of accurately predicting the DC link voltage and grid currents. Finally, Fig. 5 shows the online validation of the designed DT and compared to the physical measurement. It can be noticed that the proposed DT can accurately simulate the response of the physical system in a real-time manner.

Moreover, based on the error between sensors measurements and DT predictions, the model is updated online. This is done by considering the difference as a new state (Δx). The objective of the online updating is solely to minimize Δx using a Linear quadratic regulator (LQR). LQR is an optimal controller that is specifically used to force a specific state to diverge to zero. To this end, the outputs of the DT after the online updating can be represented as follows,

$$\begin{aligned} \tilde{\mathbf{V}}_{abc} &= \hat{\mathbf{V}}_{abc} + u_v \\ \tilde{\mathbf{I}}_{abc} &= \hat{\mathbf{I}}_{abc} + u_i \\ \tilde{V}_{dc} &= \hat{V}_{dc} + u_d \end{aligned} \tag{2}$$

where $u_v = -k\Delta\mathbf{V}_{abc}$, $u_i = -k\Delta\mathbf{I}_{abc}$, $u_d = -k\Delta V_{dc}$, and k is a positive gain and can be computed by Recatti equation.

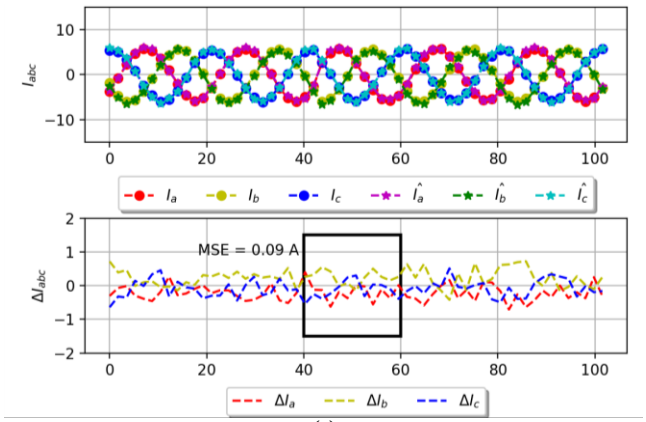


FIGURE 3. **Offline DT validation (a) steady state I_{abc}. (b) steady state V_{dc}. (c) transient I_{abc}. (d) transient V_{dc}.**

This work is licensed under a Creative Commons Attribution 4.0 License. For more information, see https://creativecommons.org/licenses/by/4.0/

This article has been accepted for publication in IEEE Open Journal of the Industrial Electronics Society. This is the author's version which has not been fully edited and content may change prior to final publication. Citation information: DOI 10.1109/OJIES.2023.3290169

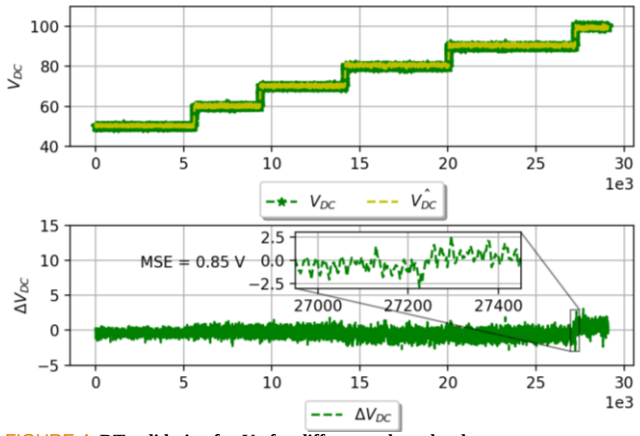


FIGURE 4. **DT validation for V_{dc} for different voltage levels.**

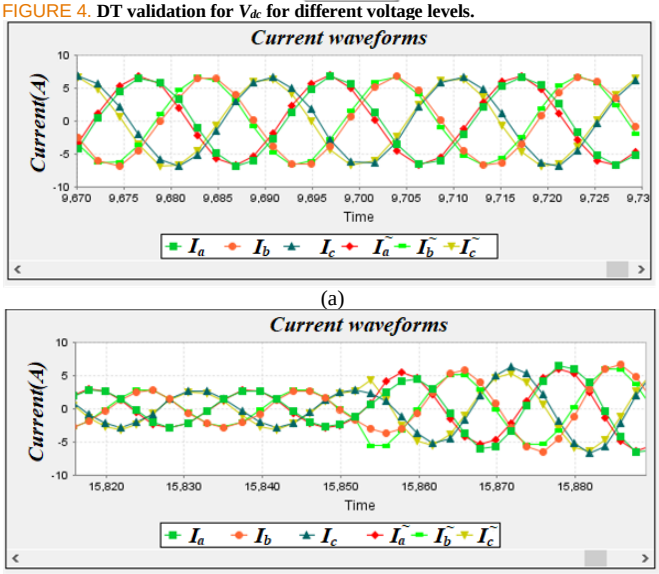


FIGURE 5. **Online experimental validation of the DT (a) Steady state validation. (b) Transient validation.**

B. Control and reference current generation for T-type rectifier

The control process of multi-level rectifiers typically aims to achieve three main objectives: i) regulation of the DC link voltage, ii) regulation of grid currents, and iii) regulation of DC side capacitors' voltages. Various controllers have been proposed in the literature to accomplish these objectives [24]. Among these methods, the sliding mode controller (SMC) stands out due to its notable advantages, including simplicity, reduced number of tunable variables, shorter computational time, and robustness against parameters variations. As a result, in this study, the sliding mode controller (SMC) is adopted as the chosen control strategy, given its favorable attributes and suitability for addressing the control requirements of the multi-level rectifier. Based on the principle of power balance between input and output, the relationship between AC and DC sides can be written as follows [25],

$$\sqrt{3}V_d I_d = \frac{V_{dc}^2}{R_L} \tag{3}$$

where V_d and I_d are d-terms of grid voltage and current represented in dq frame.

The input power is written as a function of the d-term only as the q-term will be almost zero if the controller is well-designed and the source grid is operating in normal conditions. To fulfill the first objective (DC link voltage regulation), the reference currents (I_d^*) must be generated such that it ensures the divergence of V_{dc} to the reference DC link voltage (V_{dc}^*). As a result, Eq. (3) can be written as a function of the reference signals,

$$I_d^* = \frac{V_{dc}^{*2}}{\sqrt{3}V_d R_l} \tag{4}$$

Then, the grid currents can be controlled using SMC [26] by selecting the sliding surface based on the error of grid currents tracking as follows,

$$\mathbf{S}_{abc} = \mathbf{I}_{abc} - \mathbf{I}_{abc}^* \tag{5}$$

where,

$$I_a^* = I_d^* \cos(wt) \tag{6}$$

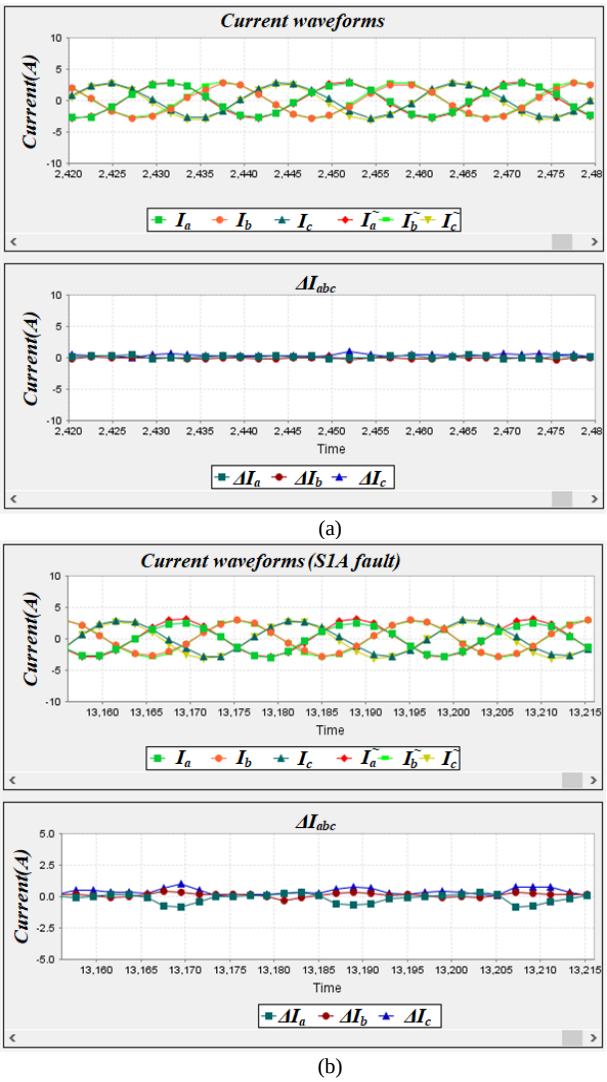
$$I_b^* = I_d^* \cos(wt + 2\pi/3) \tag{7}$$

$$I_c^* = I_d^* \cos(wt - 2\pi/3) \tag{8}$$

The sliding surface of Eq. (5) ensures the divergence of the current tracking error to zero which represents the second objective. To fulfill the DC side capacitors' voltages balancing requirement, it is worth selecting the control law as a function of the selected sliding surface and the difference between DC side capacitors' voltages (ΔV_c) as follows,

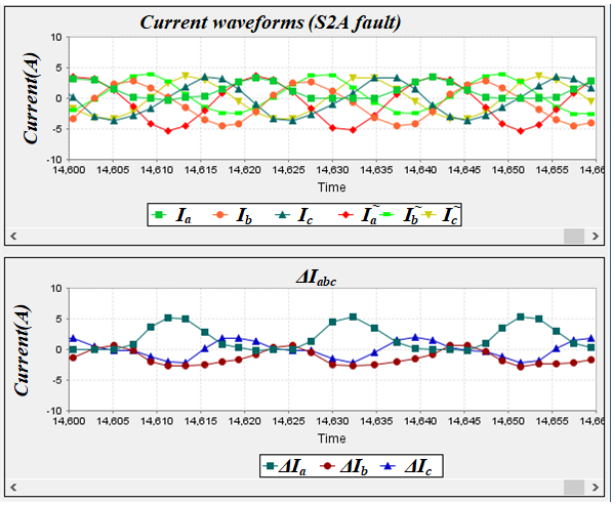
$$\mathbf{u}_{abc} = \mathbf{S}_{abc} + k\Delta V_c \tag{9}$$

where k is a 3×1 symmetrical-positive constant gain.

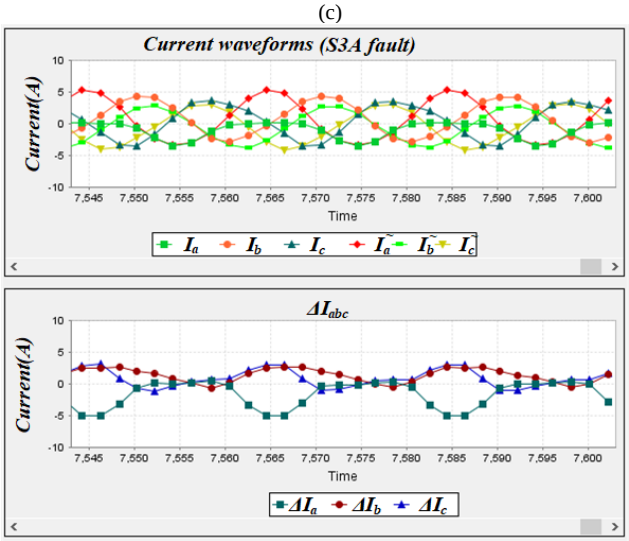


This work is licensed under a Creative Commons Attribution 4.0 License. For more information, see https://creativecommons.org/licenses/by/4.0/

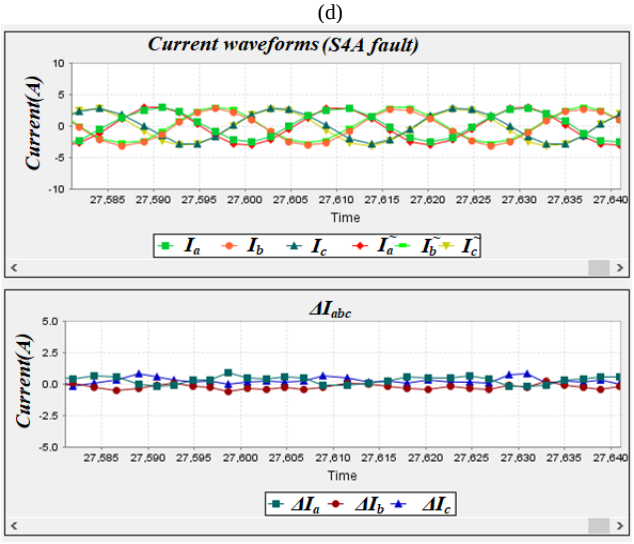
This article has been accepted for publication in IEEE Open Journal of the Industrial Electronics Society. This is the author's version which has not been fully edited and content may change prior to final publication. Citation information: DOI 10.1109/OJIES.2023.3290169



(c)



(d)



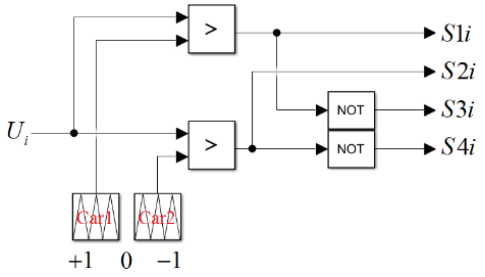
(e)

FIGURE 6. **Experimental results for ΔI_{abc} during different scenarios of faults. (a) No faults. (b) S1A fault. (c) S2A fault. (d) S3A fault. (e) S4A fault.**

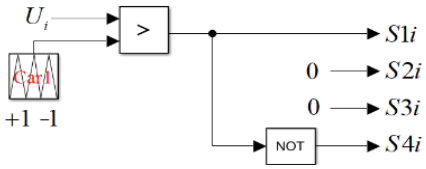
III. Implementation of the fault detection methods

A. Open-Switch Fault Detection

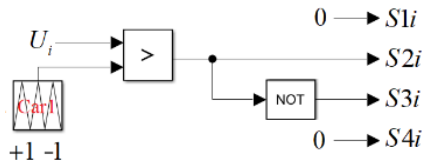
During normal operation, the current measurements and the currents obtained from the DT are almost the same, and the error between them ($\Delta \mathbf{I}_{abc}$) approaches zero. During the open-switch faults, each switch generates a specific and repeatable



(a)



(b)



(c)

FIGURE 7. **Switching functions. (a) Normal switching function. (b) Switching function for S2i and S3i faults. (c) Switching function for S1i and S4i faults.**

pattern of grid currents as shown in Fig. 6. The main switches (S1A and S4A) slightly affect the grid currents of the physical system, and small $\Delta \mathbf{I}_{abc}$ appears. By contrast, the secondary switches (S2A and S3A) deteriorate the quality of the grid currents, and a huge $\Delta \mathbf{I}_{abc}$ appears. It can be noticed from Fig. 6a that $\Delta \mathbf{I}_{abc}$ approaches zero during the normal operation. However, when the fault occurs in S1A, the negative error peaks appear in phase A. Similarly, S4A fault slightly increases the positive error peak of phase A, S3A significantly increases the negative error peaks of phase A, and S2A significantly increases the positive error peaks of phase A. Moreover, the same sequence is obtained for the other phases. Therefore, it can be concluded that each open-switch fault will increase the current error of its phase in a specific pattern. The obtained patterns are summarized in Table I, where (L^+) represents the location of the maximum positive error peak and (L^-) represents the location of the minimum error peak. The obtained patterns for each open-switch fault scenario convert the problem of OSF detection and localization into a simple linear comparison. Once the OSF is detected and localized, multiple methods can be used to perform tolerant control such as [27]. Normally, the T-type converter is operated using the switching function shown in Fig. 7a. Once the open-switch fault is detected and localized, an alternative switching function is used to tolerate the fault. If the OSF is detected in the secondary switches of the i^{th} leg, the gate signals of the secondary switches will be deactivated, and the main switches will be driven using the switching function shown in Fig. 7b. Finally, if the OSF is detected in the main switches, the main switches signals will be disabled, and the secondary switches will be operated by the switching function shown in Fig. 7c. The flow chart of OSF detection and localization is shown in Fig. 8.

This work is licensed under a Creative Commons Attribution 4.0 License. For more information, see https://creativecommons.org/licenses/by/4.0/

This article has been accepted for publication in IEEE Open Journal of the Industrial Electronics Society. This is the author's version which has not been fully edited and content may change prior to final publication. Citation information: DOI 10.1109/OJIES.2023.3290169

TABLE I. FAULT DETECTION AND LOCALIZATION LOOKUP TABLE

L^+	L^-	Fault
A	-	S2A
B	-	S2B
C	-	S2C
-	A	S3A
-	B	S3B
-	C	S3C

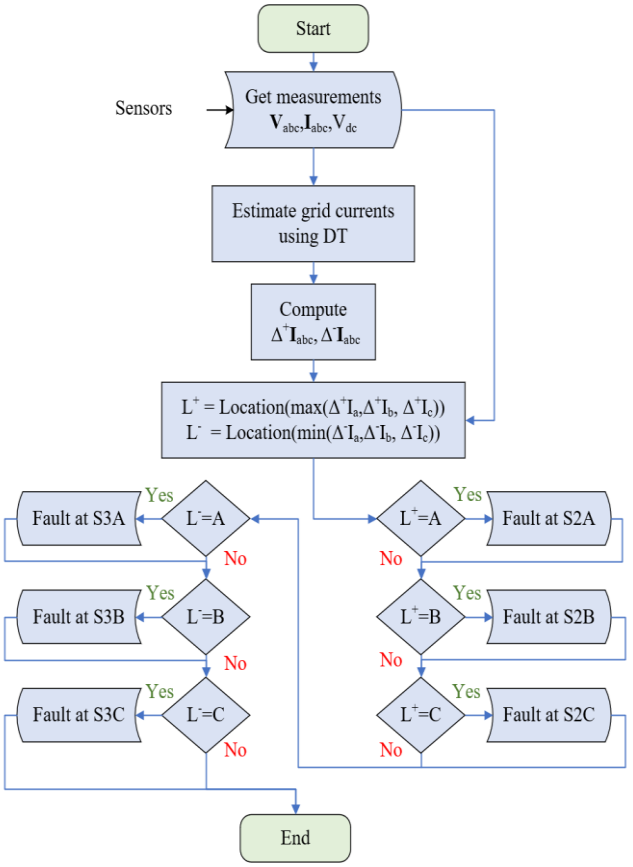


FIGURE 8. **Open-switch fault detection algorithm flow chart.**

B. Sensorless control and sensors fault tolerant

The designed DT can be used for the sensorless control in case of the decision to have the sensorless mode to be the only solution. At the same time, the DT can be used and integrated with the physical sensors to provide the required feedback signals in case of sensors failure. The first solution would provide significant benefits such as adaptability to the environment, lower cost, and reduced space requirements, while the second one increases the reliability of the controlled system.

Normally, the inputs of the physical system ($\mathbf{V}_{abc}$ and $\mathbf{U}_{abc}$) are applied to the DT, then DT provides an estimation of the physical system's outputs ($\mathbf{I}_{abc}$ and V_{dc}). Therefore, the outputs of the DT can be used for current-sensorless or fault tolerant control as shown in Fig. 9a. In this case, the DT continuously receives the voltage measurements and the control signal, then computes the corresponding grid currents and feeds them directly to the control law. On the other hand, if the current measurements are available and healthy, the inverse of the DT is activated. In this case, the DT receives the outputs of the physical system and provides the grid voltages as shown in Fig. 9b. The estimated grid voltages are used with PLL function [28] to estimate the phase angle. Finally, the flow chart of sensors fault detection is shown in Fig. 9c. The measurements are collected from the sensors and compared with the DT outputs. If the voltage difference ($\Delta\mathbf{V}_{abc}$) between voltage measurement and DT estimated voltage is larger than a specific threshold value (T_{max}), then the voltage sensors contain false or high noise.

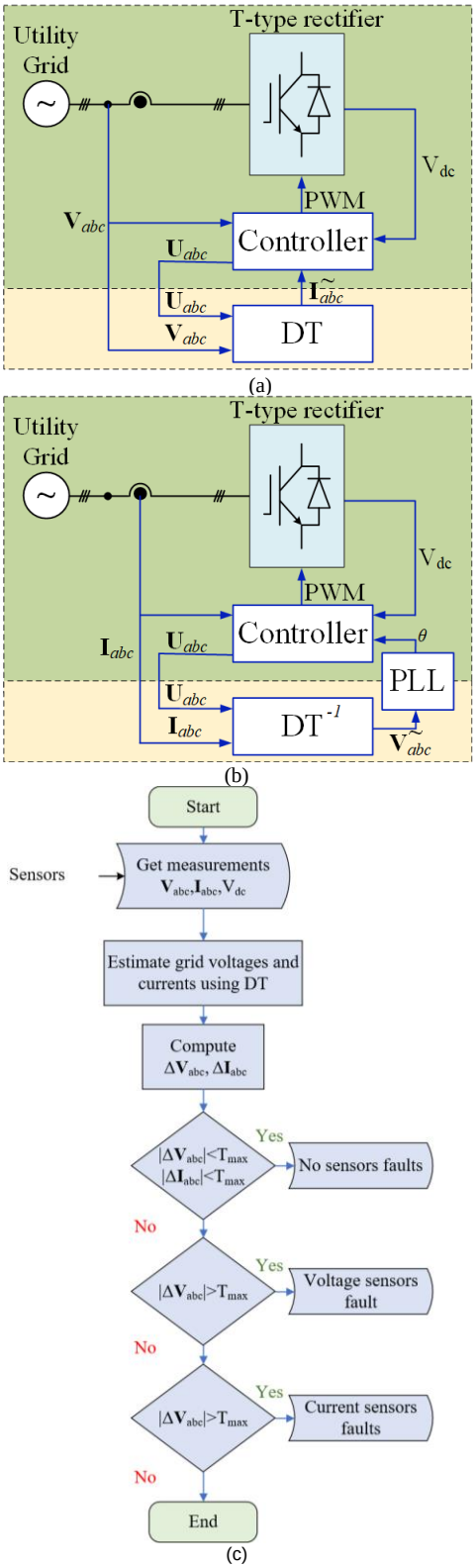


FIGURE 9. **VACSF tolerant control (a) CSF (b) VSF (c) Sensors fault detection flow chart.**

This work is licensed under a Creative Commons Attribution 4.0 License. For more information, see https://creativecommons.org/licenses/by/4.0/

This article has been accepted for publication in IEEE Open Journal of the Industrial Electronics Society. This is the author's version which has not been fully edited and content may change prior to final publication. Citation information: DOI 10.1109/OJIES.2023.3290169

Therefore, the estimated grid voltages vector will be considered as feedback instead of the physical measurements. Similarly, if the current difference ($\Delta \mathbf{I}_{abc}$) is larger than T_{max}, the system will consider the estimated currents vector as a feedback signal.

IV. Experimental results

The experimental implementation of the Digital Twin, open-switch fault diagnosis, sensorless control, and sensor fault tolerance was conducted using the STM32H745 microcontroller. This microcontroller, known for its cost-effectiveness, features a dual-core architecture comprising the H7 and M4 cores. The control loop, fault-tolerant algorithms, and grid synchronization functions were implemented on the H7 core. On the other hand, the M4 core was responsible for the offline Digital Twin model, online updating of the Digital Twin, and measurements acquisition. This division of tasks between the two cores optimized the utilization of resources and facilitated efficient execution of the proposed methodologies.

The proposed methods are applied to a lab-scale T-type rectifier as shown in Fig. 10. The setup consists of MX30 grid emulator to provide the input power, L-input filter, T-type rectifier, Tektronix oscilloscope, and programmable electrical load (Chroma 63084). All parameters used in these experiments are shown in Table II.

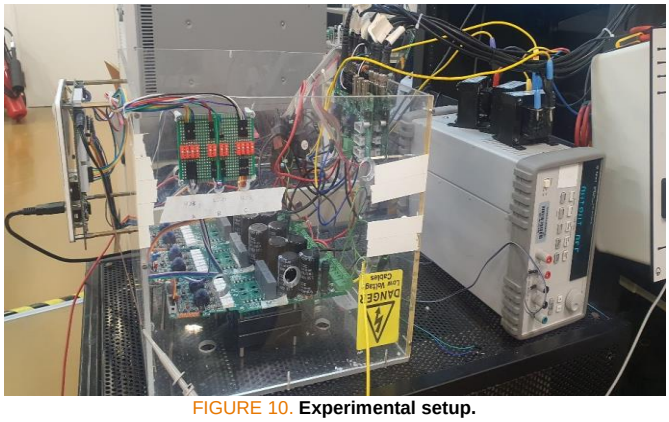


FIGURE 10. **Experimental setup.**

TABLE II. FAULT DETECTION AND LOCALIZATION LOOKUP TABLE

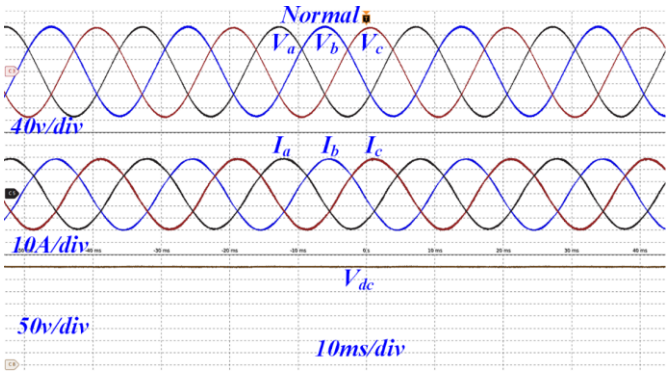
Symbol	*Value*	*Symbol*	*Value*
$\mathbf{V}_{abc}$	*110Vrms*	C_L	$2200\mu F$
L_g	*1mH*	R_L	*25-50*Ω
R_g	1m Ω	T_s	$10\mu s$

A. Open-switch faults tolerant experimental results

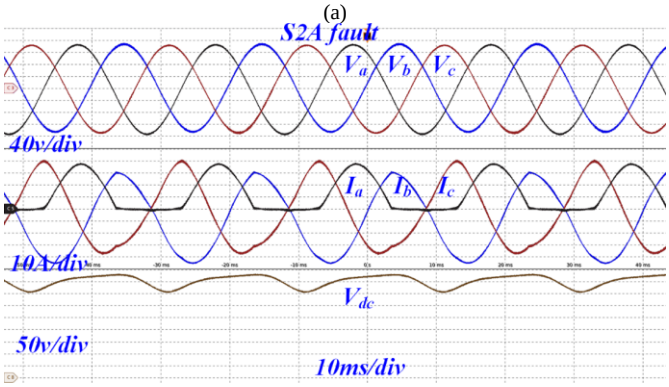
The first experiment shows the response of the proposed OSF detection and tolerant algorithm. Fig. 11(a) shows the response of the system under healthy conditions. It can be noticed that the grid currents are sinusoidal and in phase with the grid voltages which means a unity power factor is obtained. Then, an intentional OSF is applied to S2A using a manual switch and the results without and with fault tolerant control are shown in Fig. 11b and c respectively.

It can be noticed that the response of the system has deteriorated when S2A OSF exists. The currents are increased, become out of phase with the grid voltages, and become highly distorted. Moreover, the ripple of the DC link voltage is dramatically increased. However, when the tolerant control is enabled, the proposed algorithm allows the system to operate safely and satisfactorily.

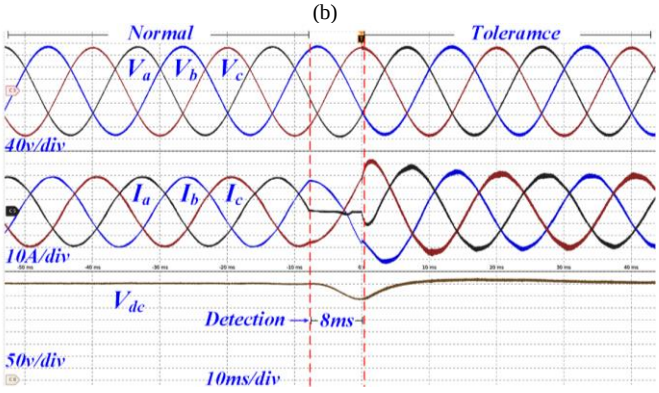
The quality of grid currents is restored, the ripples of the DC link voltage have vanished, and the unity power factor is restored. Similarly, the results of S3B OSF are shown in Fig. 11(d) and (e). For both faults, the detection and tolerant of the faults are done very fast within 8ms. Moreover, the algorithm was validated for all 12 switches, and the same results were obtained. However, only the results of S2A and S3B were added to avoid paper overlength.



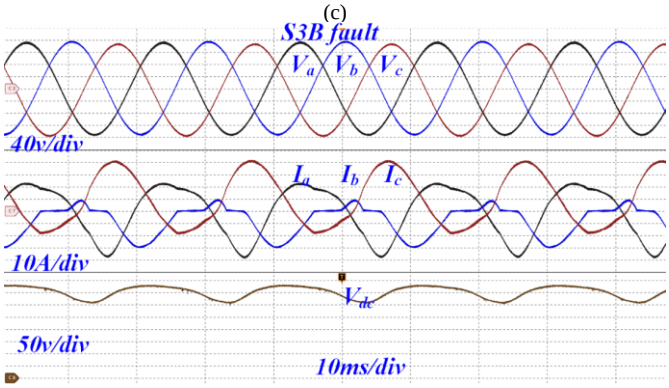
(a)



(b)



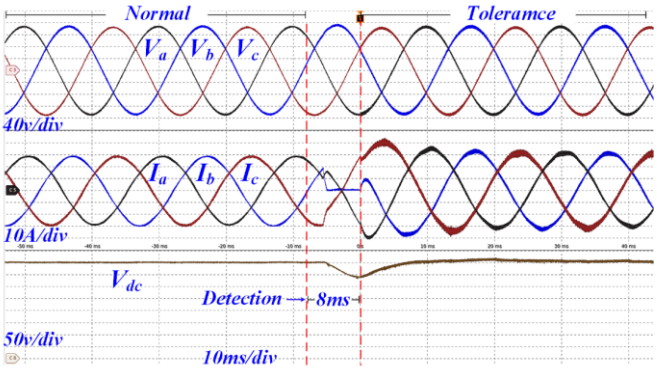
(c)



(d)

This work is licensed under a Creative Commons Attribution 4.0 License. For more information, see https://creativecommons.org/licenses/by/4.0/

This article has been accepted for publication in IEEE Open Journal of the Industrial Electronics Society. This is the author's version which has not been fully edited and content may change prior to final publication. Citation information: DOI 10.1109/OJIES.2023.3290169

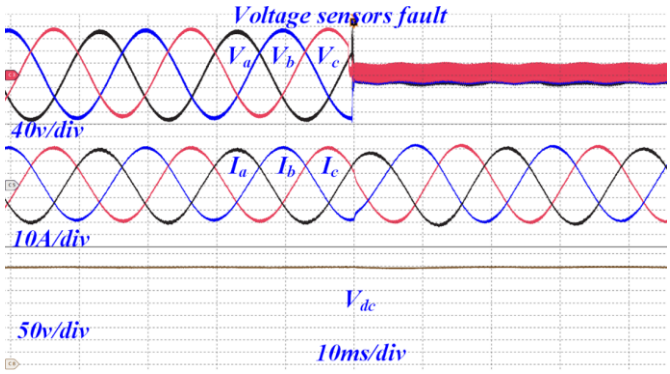


(e)

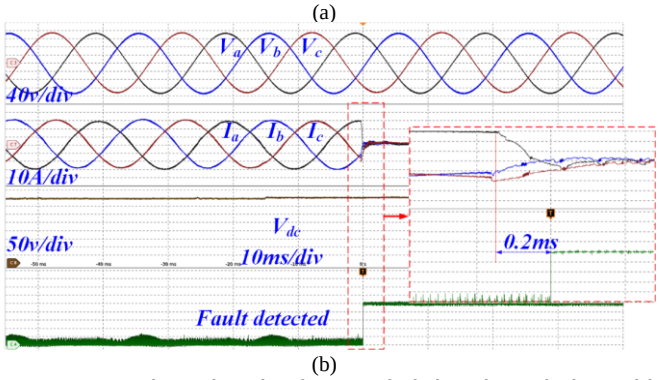
FIGURE 11. **Experimental results of fault detection and tolerant. (a) Normal operation. (b) S2A fault without OSF detection and tolerant. (c) S2A fault tolerant. (d) S3B fault without OSF detection and tolerant. (c) S2B fault tolerant.**

B. Sensors fault tolerant experimental results

The proposed DT-based fault tolerant control is validated under voltage and current sensors faults. This experiment is done by disconnecting the sensors during the online operation of the physical system. Fig. 12a shows the response of the physical system when the voltage sensors fail, while Fig. 12b shows the response when the current sensors fail. When the voltage sensors fail, the grid currents are slightly affected for a short time (< 1 ms). This time represents the transient period between sensored and sensorless control. However, the quality of the grid currents is restored immediately after enabling the inverse of the digital twin. Similarly, when the current sensors fail, the DT is able to provide real-time currents feedback and feed them to the control algorithm. It can be noticed that the current sensors faults are detected and tolerated within 0.2 ms, which can be considered one of the fastest detection algorithms. In both cases, the DC link voltage is almost not affected and remains constant all the time.



(a)



(b)

FIGURE 12. **Experimental results of sensors fault detection and tolerant. (a) voltage sensors fault tolerant. (b) current sensors fault tolerant**.

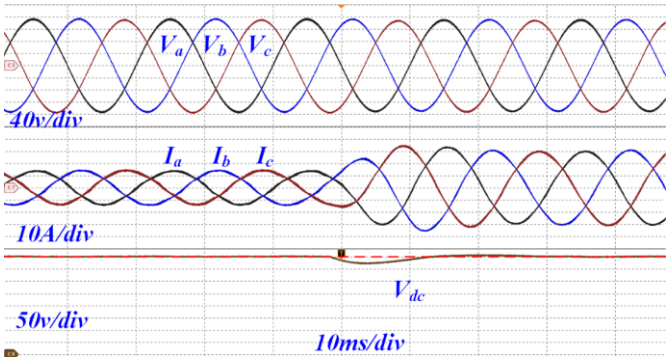


FIGURE 13. **Experimental results of voltage-sensorless control during sudden load change.**

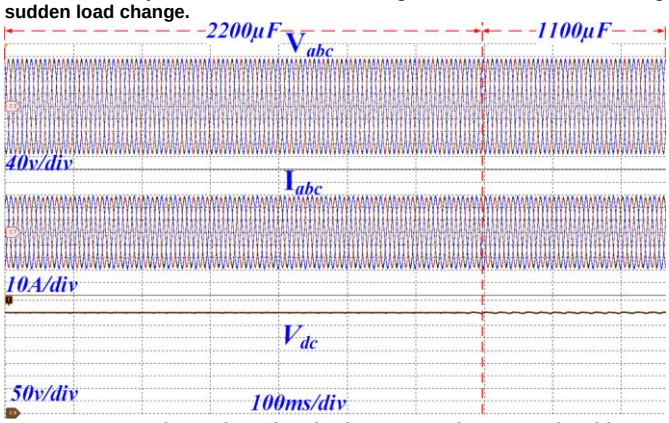


FIGURE 14. **Experimental results of voltage-sensorless control sudden DC side capacitance change.**

C. Sensorless control with severe parameters uncertainty experimental results

To demonstrate the robustness of the proposed techniques against parameters uncertainty, two experiments were performed under highly uncertain conditions. To further enhance the level of challenge, these experiments were conducted in voltage sensorless control mode.

In the first experiment, a sudden doubling of the load was induced by reducing the load resistance from 50Ω to 25Ω. The outcomes of this experiment, illustrating the results obtained from the sudden load change, are presented in Figure 13.

Upon doubling the load, the DC link voltage experiences a drop of 6.25%. However, this voltage drop is rapidly compensated within 10ms, exhibiting minimal overshoot or ripples. Likewise, the grid currents promptly and smoothly adjust to the new load conditions. Although a slight amount of overshoot temporarily occurs due to the significant level of uncertainty in the model, the grid currents converged swiftly to their correct values, benefiting from the online updating of the Digital Twin (DT).

Considering that capacitors are vulnerable components in power electronic systems, prone to rapid degradation or even complete failure, it is crucial to assess the effectiveness of the proposed methods under such severe conditions. In order to demonstrate the effectiveness of the proposed techniques, the DC side capacitance is reduced online from 2200µF to 1100µF experimentally without changing any parameter in the DT or the SMC. The obtained results from this experiment are depicted in Figure 14. It can be observed that the grid currents remain largely unaffected by the capacitance change, while a minor ripple emerges in the DC link voltage with a magnitude of V_{rpp}<2%. Notably, despite the significant alteration in

This work is licensed under a Creative Commons Attribution 4.0 License. For more information, see https://creativecommons.org/licenses/by/4.0/

This article has been accepted for publication in IEEE Open Journal of the Industrial Electronics Society. This is the author's version which has not been fully edited and content may change prior to final publication. Citation information: DOI 10.1109/OJIES.2023.3290169

capacitance, the ripple of the DC link voltage remains within the limits set by international standards.

These experiments serve as compelling evidence of the validity and robustness of the proposed DT-based sensorless control approach in dealing with severe parameter uncertainties and sudden changes in the system.

V. CONCLUSION

A novel faults detection and fault tolerant control method was proposed in this paper for a three-phase T-type rectifier based on digital twin technology. The proposed method was able to accurately simulate the dynamic behavior of the T-type rectifier in addition to its ability to provide detailed information and feedback signals of the physical system. The proposed DT, fault detection, and tolerant techniques were designed, analyzed, and implemented on a lab-scale prototype to show the validity of the proposed method. The obtained results showed the correctness and high-speed response of both proposed fault detection and fault tolerant control. Open switch faults were detected and tolerated within 8ms while the sensors faults were detected and tolerated within 0.2ms. Moreover, the proposed method is applicable for many kinds of power converters including AC-DC converters, DC-DC converters, and DC-AC converters for both two-level and multi-level converters.

VI. Acknowledgment

This publication was made possible by NPRP12C-33905- SP-213 from the Qatar National Research Fund (a member of Qatar Foundation). The statements made herein are solely the responsibility of the authors.

References

[1]S. Mihai *et al.*, "Digital twins: a survey on enabling technologies, challenges, trends and future prospects," *IEEE Communications Surveys & Tutorials*, 2022.

[2]S. Milovanović, S. Strobl, P. Ladoux, and D. Dujić, "Hardware-in-the-loop modeling of an actively fed mvdc railway systems of the future," *IEEE Access*, vol. 9, pp. 151493-151506, 2021.

[3]P. Jain, J. Poon, J. P. Singh, C. Spanos, S. R. Sanders, and S. K. Panda, "A digital twin approach for fault diagnosis in distributed photovoltaic systems," *IEEE Transactions on Power Electronics*, vol. 35, no. 1, pp. 940-956, 2019.

[4]M. Milton, C. De La O, H. L. Ginn, and A. Benigni, "Controller-embeddable probabilistic real-time digital twins for power electronic converter diagnostics," *IEEE Transactions on Power Electronics*, vol. 35, no. 9, pp. 9850-9864, 2020.

[5]Y. Peng, S. Zhao, and H. Wang, "A digital twin based estimation method for health indicators of DC–DC converters," *IEEE Transactions on Power Electronics*, vol. 36, no. 2, pp. 2105-2118, 2020.

[6]A. Sharida, S. Bayhan, and H. Abu-Rub, "Fault-Tolerant Self-Tuning Control for Three-Phase Three-Level T-type Rectifier," *IEEE Transactions on Power Electronics*, vol. 38, no. 6, pp. 1-10, 2023.

[7]Z. Xing, Y. He, and W. Zhang, "An Online Multiple Open-Switch Fault Diagnosis Method for T-type Three-level Inverters Based on Multi-modal Deep Residual Filter Network," *IEEE Transactions on Industrial Electronics*, 2022.

[8]P. Mehta, S. Sahoo, and M. Kumar, "A fault‐diagnosis and tolerant control technique for five‐level cascaded H‐bridge inverters," *IET Circuits, Devices & Systems*, vol. 15, no. 4, pp. 366-376, 2021.

[9]S.-H. Kim, S.-M. Kim, S. Park, and K.-B. Lee, "Switch open-fault detection for a three-phase hybrid active neutral-point-clamped rectifier," *Electronics*, vol. 9, no. 9, p. 1437, 2020.

[10]M. Chen and Y. He, "Open-circuit fault diagnosis method in NPC rectifiers using fault-assumed strategy," *IEEE Transactions on Power Electronics*, vol. 37, no. 11, pp. 13668-13683, 2022.

[11]J.-S. Lee and K.-B. Lee, "Open-circuit fault-tolerant control for outer switches of three-level rectifiers in wind turbine systems," *IEEE Transactions on Power Electronics*, vol. 31, no. 5, pp. 3806-3815, 2015.

[12]S. Bayhan, "Grid voltage sensorless model predictive control for a single-phase T-Type rectifier with an active power decoupling circuit," *IEEE Access*, vol. 9, pp. 19161-19174, 2021.

[13]H. Makhamreh, M. Trabelsi, O. Kükrer, and H. Abu-Rub, "A lyapunov-based model predictive control design with reduced sensors for a puc7 rectifier," *IEEE Transactions on Industrial Electronics*, vol. 68, no. 2, pp. 1139-1147, 2020.

[14]A. Rahoui, A. Bechouche, H. Seddiki, and D. O. Abdeslam, "Virtual flux estimation for sensorless predictive control of PWM rectifiers under unbalanced and distorted grid conditions," *IEEE Journal of Emerging and Selected Topics in Power Electronics*, vol. 9, no. 2, pp. 1923-1937, 2020.

[15]J. Kukkola and M. Hinkkanen, "State observer for grid-voltage sensorless control of a converter under unbalanced conditions," *IEEE Transactions on Industry Applications*, vol. 54, no. 1, pp. 286-297, 2017.

[16]V. Miskovic, V. Blasko, T. M. Jahns, A. H. Smith, and C. Romenesko, "Observer-based active damping of LCL resonance in grid-connected voltage source converters," *IEEE Transactions on Industry Applications*, vol. 50, no. 6, pp. 3977-3985, 2014.

[17]H. Yang, Y. Zhang, J. Liang, J. Gao, P. D. Walker, and N. Zhang, "Sliding-mode observer based voltage-sensorless model predictive power control of PWM rectifier under unbalanced grid conditions," *IEEE Transactions on Industrial Electronics*, vol. 65, no. 7, pp. 5550-5560, 2017.

[18]H.-C. Chen and J.-Y. Liao, "Bidirectional current sensorless control for the full-bridge AC/DC converter with considering both inductor resistance and conduction voltages," *IEEE Transactions on Power Electronics*, vol. 29, no. 4, pp. 2071-2082, 2013.

[19]S. Bayhan and H. Komurcugil, "A current sensorless control method for multi‐level active front‐end rectifiers with LCL filter," *IET Power Electronics*, 2022.

[20]E. Mohammadi, M. Alizadeh, M. Asgarimoghaddam, X. Wang, and M. G. Simões, "A review on application of artificial intelligence techniques in microgrids," *IEEE Journal of Emerging and Selected Topics in Industrial Electronics*, 2022.

[21]M. Alrifaey *et al.*, "Hybrid deep learning model for fault detection and classification of grid-connected photovoltaic system," *IEEE Access*, vol. 10, pp. 13852-13869, 2022.

[22]K. Sun, W. Qiu, W. Yao, S. You, H. Yin, and Y. Liu, "Frequency injection based HVDC attack-defense control via squeeze-excitation double CNN," *IEEE Transactions on Power Systems*, vol. 36, no. 6, pp. 5305-5316, 2021.

[23]M. Fahim, V. Sharma, T.-V. Cao, B. Canberk, and T. Q. Duong, "Machine learning-based digital twin for predictive modeling in wind turbines," *IEEE Access*, vol. 10, pp. 14184-14194, 2022.

[24]H. Komurcugil, S. Bayhan, R. Guzman, M. Malinowski, and H. Abu-Rub, *Advanced Control of Power Converters: Techniques and Matlab Simulink Implementation* (no. 1). Wiley-IEEE Press, 2023.

[25]H. Komurcugil, S. Bayhan, and M. Malinowski, "Passivity-based control strategy with improved robustness for single-phase three-level T-type rectifiers," *IEEE Access*, vol. 9, pp. 59336-59344, 2021.

[26]S. Bayhan and H. Komurcugil, "Sliding-mode control strategy for three-phase three-level T-type rectifiers with DC capacitor voltage balancing," *IEEE Access*, vol. 8, pp. 64555-64564, 2020.

[27]B. Long, T. Cao, D. Sheng, J. Rodriguez, J. M. Guerrero, and K. T. Chong, "Sequential Model Predictive Fault-Tolerance Control for T-Type Three-Level Grid-Connected Converters With LCL Filters," *IEEE Transactions on Industrial Electronics*, vol. 69, no. 9, pp. 9039-9051, 2021.

[28]S. S. Refaat, O. Ellabban, S. Bayhan, H. Abu-Rub, F. Blaabjerg, and M. Begovic, *Smart Grid and Enabling Technologies*. John Wiley & Sons, 2021.



Ali Sharida Received the B.E. degree in Mechatronics engineering from Palestine Technical University (PTUK), Tulkarm, Palestine, in 2013, and the M.Sc. degrees in Mechatronics engineering from Palestine Polytechnic University (PPU), Hebron, Palestine, in 2020. In 2014 he joined PTUK as a T.A. In 2022, worked at Texas A&M University at Qatar



Sertac Bayhan (Senior Member, IEEE) received the MS and PhD degrees in electrical engineering from Gazi University, Ankara, Turkey, in 2008 and 2012, respectively. His undergraduate studies also at the same university and he graduated as valedictorian. His research encompasses power electronics and their applications in next-generation power and energy systems, including

This work is licensed under a Creative Commons Attribution 4.0 License. For more information, see https://creativecommons.org/licenses/by/4.0/

This article has been accepted for publication in IEEE Open Journal of the Industrial Electronics Society. This is the author's version which has not been fully edited and content may change prior to final publication. Citation information: DOI 10.1109/OJIES.2023.3290169

as an Associate Research Assistant. In the same year, he enrolled to Texas A&M as a Ph.D. student. His current research interests include intelligent systems, systems identification, power converters, power converters control, and adaptive control.



Naheel Faisal Kamal received B.S. and M.S. degrees in Computer Engineering from Qatar University in 2019 and 2021 respectively. He worked on multiple research projects as a research assistant and as a teaching assistant in the College of Computer Engineering at Qatar University. He is currently a Ph.D. student at Texas A&M University and a research graduate assistant at Texas A&M University at Qatar. His research focuses on the privacy and security of the smart grid and electric vehicle charging communication systems.



Hussein Alnuweiri (S'81–M'83–SM'17) received the PhD degree in electrical and computer engineering from the University of Southern California, Los Angeles, in 1989. Currently, he is a professor with the Electrical and Computer Engineering Program at Texas A&M University at Qatar. Prior to 2007, he was a professor in the Department of Electrical and Computer Engineering at University of British Columbia in Vancouver, BC, Canada. From 2000 to 2006, he served as a Canadian Delegate to the ISO/IEC JTC1/SC29 Standards Committee (MPEG-4 Multimedia Delivery), where he worked within the MPEG-4 standardization JTC1-SC29WG11 group where he contributed one of the first client-server video streaming reference software. He has a long record of industrial collaborations with several major companies worldwide. He is also an inventor and holds four US patents. He has authored or co-authored more then 250 refereed journal and conference papers in various areas of computer and communications research. In particular, his research interests include: intelligent IoT systems, digitalization, digital twin technologies, Internet computing, and mobile cloud computing.

renewable energy integration, electrified transportation, and demand-side management. Dr. Bayhan has acquired $13M in research funding and published more than 170 papers in mostly prestigious IEEE journals and conferences. He is also the coauthor of three books and six book chapters. He currently serves as Associate Editor for Transactions on Industrial Electronics, IEEE Journal of Emerging and Selected Topics in Industrial Electronics, IEEE Open Journal of the Industrial Electronics Society, and IEEE Industrial Electronics Technology News, and Guest Editor for the IEEE Transactions on Industrial Informatics.



Haitham Abu-Rub (Fellow, IEEE) received the M.Sc. degree from Gdynia Maritime Academy, Gdynia, Poland, 1990, and the Ph. D. degree from Technical University of Gdansk, Poland, in 1995, all in electrical engineering. He also holds another Ph.D. degree from Gdansk University, Gdansk, Poland, in 2004, in humanities. Since 2006, he has been with Texas A&M University at Qatar, Doha, Qatar, where he is currently a Professor and Managing Director of the Smart Grid Center Extension. His main research interests are energy conversion systems, smart grid, renewable energy systems, electric drives, and power electronic converters. Dr. Abu-Rub is the recipient of many prestigious national and international awards and recognitions, such as the American Fulbright Scholarship and the German Alexander von Humboldt Fellowship. He has co-authored more than 550 journal and conference papers, six books, and six book chapters. Dr. Abu-Rub is an IEEE Fellow and Co-Editor in Chief of the IEEE Transactions on Industrial Electronics.

This work is licensed under a Creative Commons Attribution 4.0 License. For more information, see https://creativecommons.org/licenses/by/4.0/